JACS
JOURNAL OF THE AMERICAN CHEMICAL SOCIETY

COMMUNICATION

pubs.acs.org/JACS

Dithienogermole As a Fused Electron Donor in Bulk Heterojunction Solar Cells

Chad M. Amb,[‡] Song Chen,[†] Kenneth R. Graham,[‡] Jegadesan Subbiah,[†] Cephas E. Small,[†] Franky So,*[,†] and John R. Reynolds*[,‡]

[†]Department of Materials Science and Engineering and [‡]The George and Josephine Butler Polymer Research Laboratory, Department of Chemistry, Center for Macromolecular Science and Engineering, University of Florida, Box 117200, Gainesville, Florida 32611, United States

Supporting Information

ABSTRACT: We report the synthesis and bulk heterojunction photovoltaic performance of the first dithienogermole (DTG)-containing conjugated polymer. Stille polycondensation of a distannyl-DTG derivative with 1,3-dibromo-*N*-octyl-thienopyrrolodione (TPD) results in an alternating copolymer which displays light absorption extending to 735 nm, and a higher HOMO level than the analogous copolymer containing the commonly utilized dithienosilole (DTS) heterocycle. When polyDTG-TPD:$PC_{70}BM$ blends are utilized in inverted bulk heterojunction solar cells, the cells display average power conversion efficiencies of 7.3%, compared to 6.6% for the DTS-containing cells prepared in parallel under identical conditions. The performance enhancement is a result of a higher short-circuit current and fill factor in the DTG-containing cells, which comes at the cost of a slightly lower open circuit voltage than for the DTS-based cells.

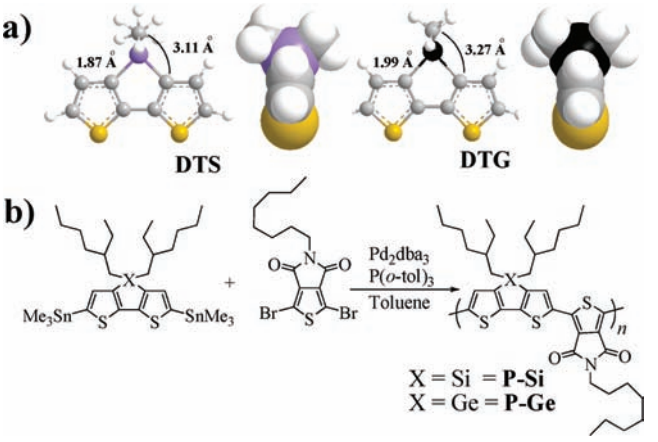

Figure 1. (a) MM2 optimized geometries of dimethyl-substituted DTS and DTG heterocycles, showing C−X bond lengths and distances of methyl groups from the nearest thienyl carbon. (b) Synthesis of **P−Si** and **P−Ge**.

Organic photovoltaics (OPVs) have been the subject of intense investigation over the past decade, as the promise of flexible, large-area cells processed using low-cost printing techniques could allow them to compete with more established semiconductor technologies.[1−3] The bulk heterojunction (BHJ) solar cell,[4] where an active light-absorbing layer consists of a mixture of a p-type material (generally a semiconducting polymer) and an n-type material (generally fullerene derivatives), has been the most successful solid-state OPV device in terms of power conversion efficiency (PCE) to date. However, these devices still exhibit fairly low PCEs compared to their inorganic counterparts, which limit their usefulness and commercial applicability. In order to take OPVs from scientific curiosities to useful products, PCEs must be increased.

Much research has been focused on the p-type light-absorbing material in BHJ cells where light absorption and HOMO−LUMO levels can be tuned as a function of repeat unit structure to maximize performance.[5−9] The donor−acceptor (D-A) approach, alternating electron-rich and electron-poor heterocycles, has been an especially successful method utilized to tune the electronic structure of these materials,[10] often employing fused heterocycles into the polymers as electron donors.[7] An example of one class of fused-ring heterocycles used in these polymers has been bithiophene systems fused by the group 14 atoms C and Si, and these molecules incorporated into polymers have given materials with high charge mobilities,[11,12] ideal for a number of organic electronic applications including BHJ solar cells.[13−16] Studies have shown that the silicon atom fusion enhances solid-state ordering compared to the carbon-fused analogue, leading to improved charge transport.[17−19] Yang and co-workers suggested that a possible reason for this behavior was that the long Si−C bonds displaced the solubilizing side chains further from the thiophene rings, allowing a stronger π-stacking interaction to occur.[19]

In our efforts to improve upon these materials, we hypothesized that the substitution of the bridging carbon or silicon atoms for the larger germanium atom would result in a further enhancement in ordering, since the long C−Ge bond lengths would further remove the bulky side chains from the planar heterocycle and allow even stronger π-stacking interactions to occur. Figure 1a shows an MM2 optimized geometry of the Si- and Ge-bridged heterocycles with methyl substituents, where the bond lengths and angles of the interior ring are consistent with single-crystal X-ray structures of known group 14 metalloles.[20] The figure shows that the C−Ge bond length is indeed longer, as the substituent methyl group is 3.11 Å away from the nearest thiophene carbon atom in DTS, whereas the methyl group is

Received: May 3, 2011
Published: June 06, 2011

dx.doi.org/10.1021/ja204056m | *J. Am. Chem. Soc.* 2011, 133, 10062–10065

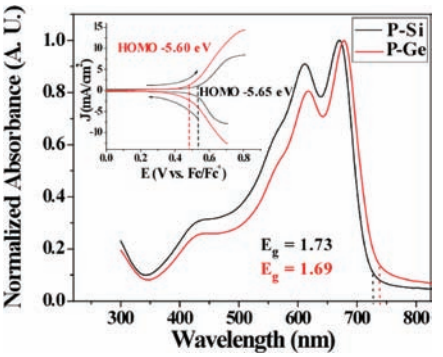

Figure 2. Thin film UV−visible absorption spectra of **P−Si** and **P−Ge** on glass. (Inset) Differential pulse voltammetry (step size 2 mV, step time 38 ms, pulse amplitude 100 mV) of thin films of **P−Si** and **P−Ge** on 0.02 cm^2 Pt disk electrodes in 0.1 M Bu_4NPF_6/acetonitrile, using a Ag/Ag^+ reference electrode (0.01 M $AgNO_3$, 0.1 M Bu_4NPF_6/acetonitrile) and Pt wire counter electrode. Arrows indicate direction of scans.

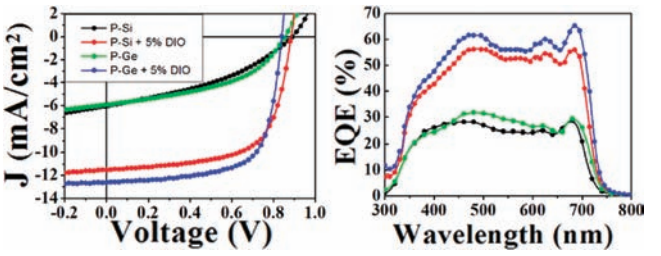

Figure 3. (Left) Illuminated $J-V$ characteristics of solar cells using ITO/ZnO/Polymer:$PC_{70}BM$ (90 nm)/MoO_3/Ag device architecture, with and without DIO as a processing additive. (Right) EQE spectra of solar cell devices utilizing **P−Si** and **P−Ge** (both 90 nm active layers).

3.27 Å from the nearest thiophene carbon in DTG. The space filling models show that the methyl groups are further displaced from the conjugated backbone, supporting the idea that the out-of plane alkyl groups can allow a larger surface for $\pi-\pi$ stacking. Interestingly, the H-atoms of the methyl groups in the DTS derivative adopt a staggered (gauche) conformation, while those in the DTG derivative are eclipsing, suggesting there is a steric relaxation as the methyl groups are moved away from one another.

In order to evaluate and compare the performance of the new DTG-containing polymer to the well-established DTS-containing polymer, we synthesized ditin-substituted DTS and DTG derivatives to be used as comonomers in Stille polymerizations with 2-ethylhexyl groups as solubilizing side chains, as shown in Figure 1b. Although we, as well as other groups, have had difficulty purifying ditin derivatives,[18,21] we found reverse-phase preparative HPLC to be an effective method of separation to give very pure ditin monomers. The C-18 functionalized, end-capped silica did not significantly remove tin groups from the DTG and DTS heterocycles in contrast to normal phase silica. Analytical HPLC chromatograms of the ditin compounds before and after preparative HPLC are shown in the Supporting Information [SI] (Figures S1−S4).

We chose to polymerize these systems with *N*-octyl-thieno-[3,4-C]pyrrole-4,6-dione, (TPD), as several groups recently showed that this acceptor results in high open circuit voltages (V_{oc}) and fill factors when incorporated in BHJ solar cell donor p-type polymers.[22−24] In particular, the Frechet group pointed out that the *N*-octyl TPD derivative gave performance superior to that of branched derivatives.[22] Also, during the course of this study, the DTS-containing copolymer **P−Si** was reported by Zhang et al.[25] and Chu et al.,[26] and will be referred to throughout this manuscript. The comonomers were polymerized using the $Pd_2dba_3/P(o\text{-tol})_3$ catalyst system, and resulted in number average (M_n) molecular weights of 31 kDa (PDI 1.7) for **P−Si** and 48 kDa (PDI 1.7) for **P−Ge** (GPC vs polystyrene, chloroform eluent). As high molecular weight has been shown to be critical for device performance,[18] preparative recycling GPC was utilized to isolate a fraction of **P−Si** with an M_n of 43 kDa (PDI 1.5) in order to make fair comparisons of device performance between polymers.

Figure 2 shows thin film UV−visible absorption spectra (drop cast from toluene solutions onto glass slides) of **P−Si** and **P−Ge**. **P−Si** gave absorption peaks at 611 and 670 nm, with an estimated bandgap of 1.73 eV, consistent with previous reports.[25,26] Upon substitution of the silicon atom for germanium in **P−Ge**, a red-shifted absorption spectrum was observed with respect to **P−Si**, with peaks at 618 and 679 nm and an estimated bandgap of 1.69 eV.

Of vital importance for BHJ solar cells are the HOMO and LUMO energy levels of the polymers, as the energy offset between p-type material HOMO and fullerene LUMO is a critical parameter in determining the open circuit voltage (V_{oc}) of the cells.[27,28] The LUMO energy is also important as sufficient driving force for electron transfer from the excited-state polymer (related to LUMO level of polymer) to PCBM is necessary for charge transfer to occur.[29,30] In order to estimate HOMO−LUMO levels from redox onsets of the polymers (for complete characterization see Figures S7−S9 in SI) thin films of **P−Si** and **P−Ge** were drop cast from toluene solutions onto Pt disk electrodes, and subsequently studied using cyclic voltammetry (CV) and differential pulse voltammetry (DPV). The oxidative differential pulse voltammagrams of **P−Si** and **P−Ge** are shown in the inset in Figure 2, demonstrating that the onset of oxidation for **P−Si** (0.53 V vs Fc/Fc^+) is about 50 mV higher than that of **P−Ge** (0.48 V vs Fc/Fc^+), giving estimated HOMO levels at −5.65 eV and −5.60 eV, respectively (assuming SCE to be −4.74 eV vs vacuum,[31] and Fc/Fc^+ to be +0.38 eV with respect to SCE).[32,33] The potentials of oxidation for **P−Si** are slightly lower than the previously reported values obtained by CV,[25,26] which is expected since DPV generally provides higher sensitivity and more well-defined redox onsets due to reductions in capacitive charging currents.[34,35] These findings are also consistent with calculated values for group 14 metalloles, where germole-containing oligomers were found to have slightly higher HOMO levels than the silole analogues.[20] The reduction potentials of the polymers are nearly identical, with both measured at −1.62 V vs Fc/Fc^+ by DPV (Figure S5 in SI) giving LUMO levels of −3.50 eV, which can be expected as the reduction potentials of the polymers are likely controlled by the TPD acceptor.

Bulk heterojunction solar cells were then fabricated using **P−Si** and **P−Ge**:$PC_{70}BM$ blends as active layers in inverted device architectures ITO/ZnO/Polymer:$PC_{70}BM$/MoO_3/Ag, and the results are presented in Figure 3. We chose to utilize the inverted geometry for device fabrication to avoid the most common problems experienced with conventional devices, such as rapid oxidation of low-work function metal cathodes and etching of ITO by the acidic PEDOT:PSS layer.[36,37] Figure 3 shows illuminated (A.M 1.5) $J-V$ curves of both polymers, with and without diiodooctane (DIO) as a processing additive.[14,38] It

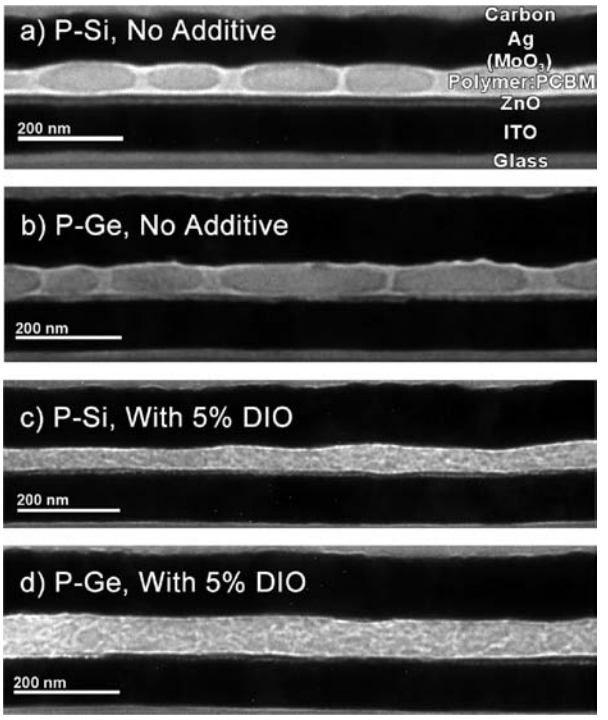

Figure 4. Cross-sectional TEM images of **P−Si**:$PC_{70}BM$ and **P−Ge**:$PC_{70}BM$-based PV cells without any additives (top) and with 5% DIO (bottom).

can be seen from Figure 3 that the performance of both polymers is greatly enhanced using 5% DIO, as both the currents and fill factors significantly increased. On optimization, **P−Si** achieved an average short-circuit current density of 11.5 mA/cm^2, an open circuit voltage of 0.89 V, and a 65% fill factor resulting in an average power conversion efficiency (PCE) of 6.6%. Although the currents and fill factors are slightly lower than those reported by Chu et al,[26] it is likely that the hole-blocking interlayer resulted in higher currents and fill factors, and also the values we report are average rather than best values. Additionally, the devices reported here are based on an inverted device architecture, whereas Chu et al.[26] utilized a standard device architecture. The DTG-containing polymer **P−Ge** gave a higher short-circuit current density (12.6 mA/cm^2) and fill factor (68%) than **P−Si**, with a lower V_{oc} of 0.85 V, for an average PCE of 7.3%. The lower V_{oc} of 40 mV for **P−Ge** is in excellent agreement with the DPV measurements, which showed that **P−Ge** has a higher HOMO level by 50 mV.

The external quantum efficiency (EQE) spectra of the devices are also shown in Figure 3, and it can be seen that without DIO both devices display fairly low quantum efficiency across the visible region. With DIO as a processing additive, the EQE of devices using **P−Si** and **P−Ge** increase dramatically, with a broad spectral response. The EQE across the visible region of **P−Ge** ranges from 55 to 65%, while that of **P−Si** ranges from 50 to 56%, with **P−Ge** also extending to longer wavelengths. This is consistent with the slightly red-shifted absorption spectrum of **P−Ge** with respect to **P−Si**.

The morphologies of the polymer:$PC_{70}BM$ blends were imaged using tapping mode atomic force micrsocopy (AFM), top-down bright field transmission electron microscopy (TEM), and cross-sectional TEM. The TEM images are all presented at similar defocus values such that the contrast between phases is enhanced without overly large fringing effects.[39] The cross-sectional TEM samples shown in Figure 4 were prepared through the use of focused ion beam (FIB) as detailed in the Supporting Information. The cross-sectional samples show the multilayer structure which consists of glass/ITO/ZnO/Polymer:PCBM/MoO_3 (too thin to be clearly observed in the TEM images)/Ag. For the cross-sectional samples an additional protective layer of carbon was deposited on top of the Ag layer, followed by a protective Pt layer.

The TEM images shown in Figures 4 and S10 (in SI) show large-scale phase separation between the polymer and $PC_{70}BM$ phases in the devices processed with no additives, with the morphologies appearing nearly identical for both polymers. AFM images (Figure S11 in SI) correlate well with the morphologies observed through TEM. Both the top down and cross-sectional TEM images shown in Figures 4 and S10 show a very similar morphology with the dark $PC_{70}BM$ domains appearing 100−350 nm in lateral dimension and ∼45−65 nm in vertical dimension. These large dimensions are much greater than typical organic exciton diffusion lengths of ∼10 nm[40,41] and thereby severely limit device performance. The low J_{SC} observed in the devices processed without DIO are attributed to this large-scale phase-separated morphology, where only a small fraction of generated excitons diffuse far enough to reach a polymer:$PC_{70}BM$ interface.

Upon addition of 5% DIO a significant reduction in phase separation is observed for both polymers. After the addition of 5% DIO, phase separation is observed to be on the order of tens of nanometers, with no large aggregates of $PC_{70}BM$ or polymer observed. This small-scale phase separation is on the order of the exciton diffusion length, and correspondingly large J_{SC} values are observed for these devices. Interestingly, the morphologies both before and after addition of DIO are nearly identical to those observed by the Janssen group for a DPP-containing polymer where a similar increase in J_{SC} was observed upon addition of DIO.[38] The cross-sectional images also show a fairly random morphology with no preferred horizontal or vertical alignment of phases. However, both top-down and cross-sectional TEM images show a fairly interconnected morphology that is necessary for efficient charge transport. The morphologies of both polymers both with and without additives appear nearly identical; thereby the performance differences of the DTG and DTS devices are likely attributed to the slightly red-shifted absorbance of the DTG analogue and possibly also to the difference in intermolecular packing.

In conclusion, we have synthesized the first dithienogermole containing conjugated polymers. The use of this heterocycle in a donor−acceptor polymer using *N*-octylthienopyrrolodione (TPD) as an acceptor results in a slightly longer wavelength absorption, and a higher HOMO level than an analogous polymer containing its dithienosilole analogue. When utilized in bulk heterojunction solar cells, the DTG-TPD copolymer **P−Ge** displays an *average* PCE of 7.3% when utilized in simple inverted device architectures without interlayers. Upon further device optimization, PCE greater than 8% is expected using **P−Ge**:$PC_{70}BM$ blends as active layers.

■ ASSOCIATED CONTENT

Supporting Information. Detailed synthetic procedures, details on solar cell fabrication, chromatographic data, electrochemical

data, TEM images, and AFM images. This material is available free of charge via the Internet at http://pubs.acs.org.

AUTHOR INFORMATION

Corresponding Author
fso@mse.ufl.edu (F.S.); reynolds@chem.ufl.edu (J.R.R.)

ACKNOWLEDGMENT

We appreciate support of this work from the AFOSR (FA9550-09-1-0320) and the ONR (N00014-11-1-0245), along with preparative GPC experiments carried out by Jimmy Deininger, and preparation of the thienopyrrolodione precursors by Coralie Richard.

REFERENCES

(1) Nielsen, T. D.; Cruickshank, C.; Foged, S.; Thorsen, J.; Krebs, F. C. *Sol. Energy Mater. Sol. Cells* **2010**, *94*, 1553.
(2) Krebs, F. C. *Sol. Energy Mater. Sol. Cells* **2009**, *93*, 394.
(3) Hoth, C. N.; Schilinsky, P.; Choulis, S. A.; Brabec, C. J. *Nano Lett.* **2008**, *8*, 2806.
(4) Yu, G.; Gao, J.; Hummelen, J. C.; Wudl, F.; Heeger, A. J. *Science* **1995**, *270*, 1789.
(5) Brabec, C. J.; Gowrisanker, S.; Halls, J. J. M.; Laird, D.; Jia, S.; Williams, S. P. *Adv. Mater.* **2010**, *22*, 3839.
(6) Scharber, M. C.; Mühlbacher, D.; Koppe, M.; Denk, P.; Waldauf, C.; Heeger, A. J.; Brabec, C. J. *Adv. Mater.* **2006**, *18*, 789.
(7) Liang, Y.; Yu, L. *Acc. Chem. Res.* **2010**, *43*, 1227.
(8) Dennler, G.; Scharber, M. C.; Brabec, C. J. *Adv. Mater.* **2009**, *21*, 1323.
(9) Thompson, B. C.; Fréchet, J. M. J. *Angew. Chem., Int. Ed.* **2008**, *47*, 58.
(10) Beaujuge, P. M.; Amb, C. M.; Reynolds, J. R. *Acc. Chem. Res.* **2010**, *43*, 1396.
(11) Tsao, H. N.; Cho, D. M.; Park, I.; Hansen, M. R.; Mavrinskiy, A.; Yoon, D. Y.; Graf, R.; Pisula, W.; Spiess, H. W.; Müllen, K. *J. Am. Chem. Soc.* **2011**, *133*, 2605.
(12) Lu, G.; Usta, H.; Risko, C.; Wang, L.; Facchetti, A.; Ratner, M. A.; Marks, T. J. *J. Am. Chem. Soc.* **2008**, *130*, 7670.
(13) Mühlbacher, D.; Scharber, M.; Morana, M.; Zhu, Z.; Waller, D.; Gaudiana, R.; Brabec, C. *Adv. Mater.* **2006**, *18*, 2884.
(14) Lee, J. K.; Ma, W. L.; Brabec, C. J.; Yuen, J.; Moon, J. S.; Kim, J. Y.; Lee, K.; Bazan, G. C.; Heeger, A. J. *J. Am. Chem. Soc.* **2008**, *130*, 3619.
(15) Peet, J.; Kim, J. Y.; Coates, N. E.; Ma, W. L.; Moses, D.; Heeger, A. J.; Bazan, G. C. *Nat. Mater.* **2007**, *6*, 497.
(16) Hou, J.; Chen, H.-Y.; Zhang, S.; Li, G.; Yang, Y. *J. Am. Chem. Soc.* **2008**, *130*, 16144.
(17) Scharber, M. C.; Koppe, M.; Gao, J.; Cordella, F.; Loi, M. A.; Denk, P.; Morana, M.; Egelhaaf, H.-J.; Forberich, K.; Dennler, G.; Gaudiana, R.; Waller, D.; Zhu, Z.; Shi, X.; Brabec, C. J. *Adv. Mater.* **2010**, *22*, 367.
(18) Coffin, R. C.; Peet, J.; Rogers, J.; Bazan, G. C. *Nat. Chem.* **2009**, *1*, 657.
(19) Chen, H.-Y.; Hou, J.; Hayden, A. E.; Yang, H.; Houk, K. N.; Yang, Y. *Adv. Mater.* **2010**, *22*, 371.
(20) Yamaguchi, S.; Itami, Y.; Tamao, K. *Organometallics* **1998**, *17*, 4910.
(21) Blouin, N.; Leclerc, M. *Acc. Chem. Res.* **2008**, *41*, 1110.
(22) Piliego, C.; Holcombe, T. W.; Douglas, J. D.; Woo, C. H.; Beaujuge, P. M.; Frechet, J. M. J. *J. Am. Chem. Soc.* **2010**, *132*, 7595.
(23) Zou, Y.; Najari, A.; Berrouard, P.; Beaupré, S.; Réda Aïch, B.; Tao, Y.; Leclerc, M. *J. Am. Chem. Soc.* **2010**, *132*, 5330.
(24) Zhang, Y.; Hau, S. K.; Yip, H.-L.; Sun, Y.; Acton, O.; Jen, A. K.-Y. *Chem. Mater.* **2010**, *22*, 2696.
(25) Zhang, Y.; Zou, J.; Yip, H. L.; Sun, Y.; Davies, J. A.; Chen, K. S.; Acton, O.; Jen, A. K.-Y. *J. Mater. Chem.* **2011**, *21*, 3895.
(26) Chu, T.-Y.; Lu, J.; Beaupré, S.; Zhang, Y.; Pouliot, J.-R.; Wakim, S.; Zhou, J.; Leclerc, M.; Li, Z.; Ding, J.; Tao, Y. *J. Am. Chem. Soc.* **2011**, *133*, 4250.
(27) Potscavage, W. J.; Sharma, A.; Kippelen, B. *Acc. Chem. Res.* **2009**, *42*, 1758.
(28) Vandewal, K.; Tvingstedt, K.; Gadisa, A.; Inganas, O.; Manca, J. V. *Nat. Mater.* **2009**, *8*, 904.
(29) Brédas, J.-L.; Beljonne, D.; Coropceanu, V.; Cornil, J. *Chem. Rev.* **2004**, *104*, 4971.
(30) Rand, B. P.; Burk, D. P.; Forrest, S. R. *Phys. Rev. B* **2007**, *75*, 115327.
(31) Hansen, W. N.; Hansen, G. J. *Phys. Rev. A* **1987**, *36*, 1396.
(32) Pavlishchuk, V. V.; Addison, A. W. *Inorg. Chim. Acta* **2000**, *298*, 97.
(33) Cardona, C. M.; Li, W.; Kaifer, A. E.; Stockdale, D.; Bazan, G. C. *Adv. Mater.* **2011**, *23*, 2367.
(34) Bard, A. J.; Faulkner, L. R. *Electrochemical Methods: Fundamentals and Applications*, 2nd ed.; Wiley: New York, 2001.
(35) Beaujuge, P. M.; Pisula, W.; Tsao, H. N.; Ellinger, S.; Müllen, K.; Reynolds, J. R. *J. Am. Chem. Soc.* **2009**, *131*, 7514.
(36) de Jong, M. P.; van Ijzendoorn, L. J.; de Voigt, M. J. A. *Appl. Phys. Lett.* **2000**, *77*, 2255.
(37) Jørgensen, M.; Norrman, K.; Krebs, F. C. *Sol. Energy Mater. Sol. Cells* **2008**, *92*, 686.
(38) Bijleveld, J. C.; Gevaerts, V. S.; Di Nuzzo, D.; Turbiez, M.; Mathijssen, S. G. J.; de Leeuw, D. M.; Wienk, M. M.; Janssen, R. A. J. *Adv. Mater.* **2010**, *22*, E242.
(39) Moon, J. S.; Lee, J. K.; Cho, S.; Byun, J.; Heeger, A. J. *Nano Lett.* **2008**, *9*, 230.
(40) Shaw, P. E.; Ruseckas, A.; Samuel, I. D. W. *Adv. Mater.* **2008**, *20*, 3516.
(41) Scully, S. R.; McGehee, M. D. *J. Appl. Phys.* **2006**, *100*, 034907.